

Rotary Steerable Directional Drilling Stick/Slip Mitigation Control

Martin T. Bayliss, * Neilkunal Panchal, ** J. F. Whidborne **

* Schlumberger Oilfield UK Plc.
Stonehouse Technology Centre, Brunel Way
Stroudwater Business Park, Stonehouse, Gloucestershire
GL10 3SX, UK (e-mail: mbayliss@slb.com).

** Cranfield University, Bedfordshire, MK43 0AL, UK
(e-mail: n.panchal@cranfield.ac.uk, j.f.whidborne@cranfield.ac.uk)

Abstract: This paper details the online-identification-based adaptive design of a stick/slip minimization algorithm and top-drive servo control for Rotary Steerable System (RSS) directional drilling tools. Stick/slip in this context refers to the downhole angular velocity variation of the bit about a nominal value. The basic pole placement controller designs are SISO linear but recursively evaluated based on an online Recursive Least Squares (RLS) identification of the open-loop plant parameters. System architecture implications for the stated algorithm are discussed, and simulation results included with and without adaptive stick/slip mitigation.

Keywords: Directional drilling, stick/slip, rotary steerable, identification, adaptive control

1. INTRODUCTION

For Rotary Steerable System (RSS) directional drilling in the oil and gas industry, the whole drillstring is rotated from the surface by a hydraulically driven top drive (typically). This technique has become increasingly important for extended reach lateral and 3D wells. Therefore, the drillstring as a whole resembles a very long and torsionally flexible propeller shaft delivering torque to the bit downhole. This architecture is prone to torsional drillstring oscillation leading to at bit rpm variation known as stick/slip. These stick/slip oscillations can cause bit damage, drillstring failure (by fatigue at threaded joints in the drillstring) reduced V_{ROP} (rate of penetration), reduced directional control performance, inconsistent tool curvature response, and higher levels of shock and vibration downhole leading generally to premature tool failure. Therefore, a controller and associated architecture which reduces stick/slip is clearly advantageous to the oil and gas industry for RSS directional drilling.

In the literature, there are various schemes discussed for active stick/slip control, including H_∞ control (Serrarens et al. 1998, Tucker and Wang 1999), sliding mode control (Navarro-Lopez and Cortes 2007, Lin et al. 2011) and open-loop stability analysis (Abbassian and Dunayevsky 1999) leading to a qualitative system configuration guide to stick/slip mitigation. This paper presents an adaptive controller utilizing RLS parameter identification for the minimization of the phenomenon of stick/slip as observed in RSS directional drilling tools. The assumption is made that the stick/slip phenomenon is primarily characterized by a second order system representing the drillstring torsional dynamics which are excited by the top-drive input torque and downhole torque on bit. Other dynamics, such a longitudinal drillstring dynamics (bit bounce) or

whirl effects (Brett et al. 1990) are treated as unmodeled dynamics. The adaptive controllers are in the form of linear SISO feedback architectures, the gains of which are designed recursively by pole placement utilizing open-loop plant parameters identified on-line by the RLS algorithm. The objectives, therefore, of the stick/slip controller and associated servo control of the top drive is to generate a top-drive set-point rotational speed input that will have the effect of minimizing the downhole periodic variation of bit rotational speed whilst tracking a demand angular speed.

The algorithm stated in this paper only requires the drillstring model parameters to be identified online for adaptive controller design, with the torque on bit treated as a virtual control input. This simplifies the control architecture considerably. The paper also assumes downhole measurements of bit rpm and torque on bit are available at the surface by means of WDP-type (wired drillpipe) technologies (Hatch et al. 2011).

The paper starts by stating the relevant dynamics for the drillstring and the bit. The paper then moves on to present the architecture for the transient simulation which summarizes the stick/slip controller and top-drive servo control placement in the overall system architecture. The linear SISO pole placement design for the stick/slip and servo controllers are then presented along with a statement of the RLS algorithm as applied to this application. Finally, transient simulation results are presented and discussed for a operationally typical parameter set.

2. STICK/SLIP GOVERNING EQUATIONS

Here the relevant dynamics are stated both for the transient simulation and the offline linear controller design,

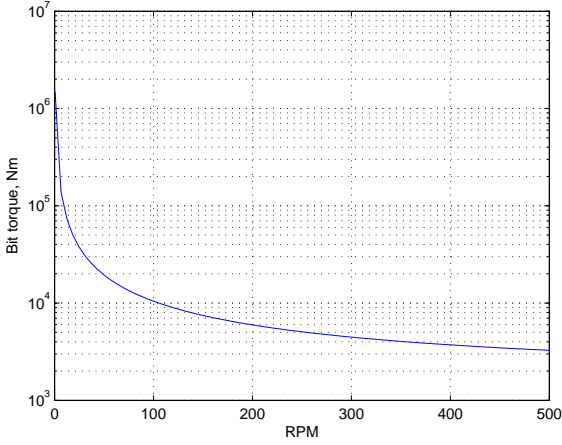


Fig. 1. T_{bit} versus RPM characteristic.

these being the V_{ROP} , torque on bit, and drillstring dynamics.

2.1 V_{ROP} dynamics

The simplified V_{ROP} dynamics are derived from a force balance of the drillstring taking into account the mass of the drillstring and the opposing viscous damping force from the bit, as summarized below:

$$M\dot{V}_{ROP} = F_{bit}, \quad (1)$$

where F_{bit} is given by the following expression (Detourney et al. 2008):

$$F_{bit} = WO B - \rho \cdot a \cdot DOC + w_a \varepsilon, \quad DOC = \frac{V_{ROP}}{\omega}, \quad (2)$$

where DOC is depth of cut and all other parameters are as defined in Table 1.

2.2 Torque on bit characteristic

Also using reference (Detourney et al. 2008) the torque on bit governing equation can be stated as follows:

$$T_{bit} = DOC \frac{\varepsilon a^2}{2} + \frac{a f w_a \varepsilon}{2}. \quad (3)$$

Of interest is the ω/T_{bit} characteristic for the bit shown in Fig. 1, which was derived using (3) and the relevant parameters stated in Table 1. It can be seen in Fig. 1 that the torque characteristic rises asymptotically as the bit speed, ω , decreases. This bit characteristic can intuitively be used to explain why the bit is the primary stick/slip excitation source. It can be appreciated that drillstring oscillations inevitably occur due to the second order lag dynamics of the drillstring (see (4)) which cause the torque on bit to slide up and down the steep torque curve as the bit rotation stops/starts, and in so doing inputs substantial torsional disturbances into the system.

2.3 Drillstring dynamics

Using the simple lumped parameter torsional model of the drillstring shown in Fig. 2 it can be deduced that the

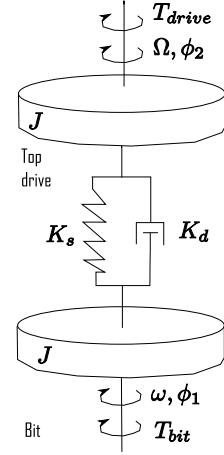


Fig. 2. Drillstring schematic showing sign conventions (note $K_s = Jc$ and $K_d = Jb$).

governing equation for the differential drillstring dynamics is

$$\ddot{\alpha} + 2D\omega_o\dot{\alpha} + \omega_o^2\alpha = \frac{1}{J}\Delta T, \quad (4)$$

where $\dot{\alpha} = \Omega - \omega$ and $\Delta T = T_{drive} - T_{bit}$. Equation (4) and Fig. 2 represent the same open-loop plant model as used by Rudat and Dashevskiy (2011) but with differing boundary conditions because the assumption that Ω is constant and that $\dot{\Omega}$ is therefore zero is not made. Hence Ω is used as the direct control input rather than $WO B$. It can be deduced from (4) that the transfer function between the differential torque and angular velocity across the drillstring is:

$$G(s) = \frac{\dot{\alpha}(s)}{\Delta T(s)} = \frac{sd}{s^2 + sb + c}, \quad (5)$$

where $d = \frac{1}{J}$, $b = 2D\omega_o$ and $c = \omega_o^2$. Equations (2), (3), and (4) can be used for the nonlinear transient simulation in a loop structure where the V_{ROP} equation will generate V_{ROP} , which in combination with w will generate a DOC , which in turn can be used to evaluate ΔT from T_{bit} and the instantaneous top-drive torque T_{drive} from the surface top-drive servo control feedback loop.

3. OVERALL SYSTEM ARCHITECTURE

With the V_{ROP} , T_{bit} , and drillstring dynamics stated in Sections 2.1, 2.2, and 2.3, the overall system architecture was implemented as shown in Fig. 3 for a transient simulation. In Fig. 3, Ω_r is the required steady state rpm for both the top drive and the downhole bit, Ω is the top-drive response, $\dot{\alpha}_v$ is the equivalent differential angular speed across the drillstring to generate the controlling virtual ΔT to regulate the stick/slip rpm amplitude to zero and Ω_u is the instantaneous summation of Ω_r and $\dot{\alpha}_v$ tracked by the top-drive servo controller.

3.1 Stick/slip adaptive controller

The top level architecture of the stick/slip controller is shown in Fig. 4 where the linear pole placed controller is designed online using the parameters identified by an RLS parameter identification algorithm (Astrom and Wittenmark 1994). The RLS algorithm recursively identifies the open-loop plant parameters for use (at a lower recursion

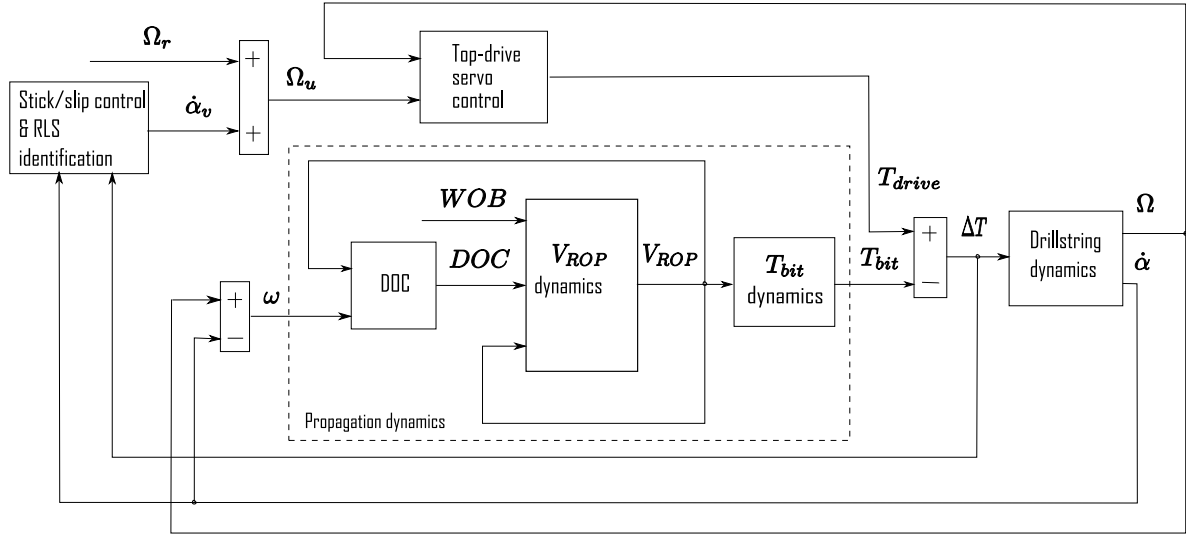


Fig. 3. Overall system architecture.

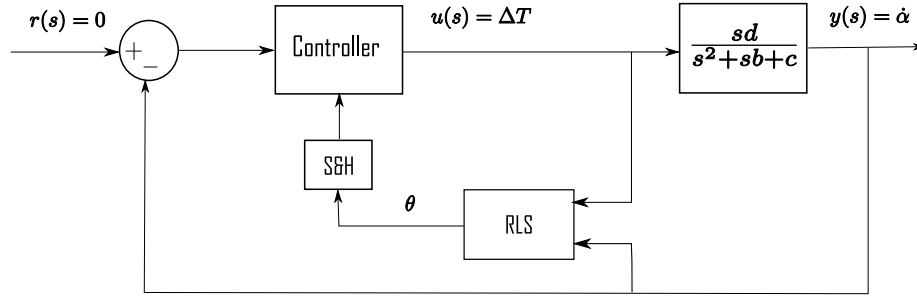


Fig. 4. Adaptive stick/slip mitigation architecture.

rate by means of a sample and hold) with the pole placement gain design detailed in Section 3.2. Note that only

the open loop plant parameters for the drillstring dynamics given by (5) are identified, and not the parameters of the torque-on bit characteristic.

Table 1. Model and controller parameters

Symbol	Description	Unit	Value
g	Controller slow pole location	s^{-1}	1.0×10^{-3}
ϱ	Bit parameter	kg/m^2	0.63
a	Bit radius	m	8.41×10^{-2}
w_a	Wear area	m^2	4.0×10^{-5}
ω	Bit angular speed	rad/s	–
ϕ_1	Bit angular position	rad	–
Ω	Top drive angular speed	rad/s	–
ϕ_2	Top drive angular position	rad	–
f	Friction factor	–	0.874
ε	Rock specific energy	J/m^3	1.0×10^9
D	Drillstring damping ratio	–	0.31
ω_o	Drillstring natural frequency	rad/s	2.0
J	Drillstring inertia	kg m^2	200.0
T_{bit}	Torque on bit	N m	–
T_{drive}	Top drive input torque	N m	–
M	Mass of drillstring	kg	2.73×10^4
WOB	Weight on bit	kN	27
b	$G(s)$ parameter	s^{-1}	0.44
c	$G(s)$ parameter	s^{-2}	4.0
d	$G(s)$ parameter	$\text{kg}^{-1}\text{m}^{-2}$	5.0×10^{-3}
S&H	Sample and hold update period	s	50
ω_{n1}	Stick/slip CL natural frequency	Hz	0.05
ω_{n2}	Servo control natural frequency	Hz	2.5
ζ	Nominal CL damping ratio	–	0.707
λ	RLS forgetting factor	–	0.99999
σ	T_{bit} noise standard deviation	N m	100

3.2 Stick/slip linear controller design

For the outer loop stick/slip controller design, the linearised open-loop transfer function given by (5) will be used with $\dot{\alpha}$ measured for feedback control (as can be seen from Figs 4 and 5). It will be noted that the open loop transfer function of the drillstring dynamics is that of a zero at the origin and a pole pair. It can be seen in Fig. 5 that a conventional nested structure has been used with integral and derivative action. However, a single slow pole, $(s + g)$, $g \ll 1$, has been added after the nested structure to approximately cancel the zero at the origin (an added pure integrator would make the system marginally stable). With this structure, the zero at the origin can be ignored, and pole placement can be used to give the system the required dynamics as follows:

$$\frac{y(s)}{r(s)} = \frac{K_i d}{s^3 + s^2(b + dK_d) + sc + K_i d}, \quad (6)$$

with the pole placed gains:

$$K_d = \frac{4\zeta^2\omega_{n1}^2 - 2b\zeta\omega_{n1} - \omega_{n1}^2 + c}{2\zeta d\omega_{n1}}, \quad (7)$$

$$K_i = \frac{\omega_{n1}(c - \omega_{n1}^2)}{2\zeta d}, \quad p = \frac{c - \omega_{n1}^2}{2\zeta\omega_{n1}}, \quad (8)$$

where p is the location of the third closed-loop pole.

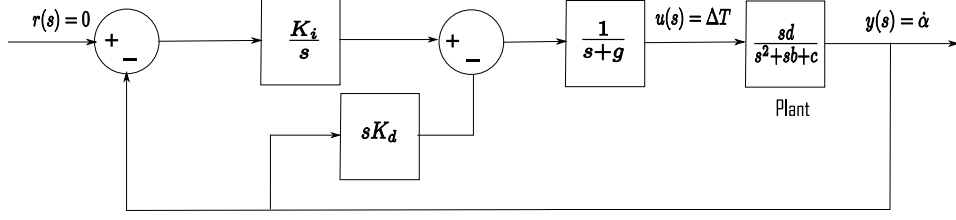


Fig. 5. Nested ID, slow pole feedback stick/slip regulator.

4. TOP-DRIVE SET POINT EVALUATION

Section 3.2 describes the architecture and design of a linear SISO feedback controller that generates ΔT across the drillstring required to make $\dot{\alpha} \rightarrow 0$. Clearly, there is no direct way to apply T_{bit} at bit to give the required ΔT . Therefore, a secondary stage to the controller is required that converts the controller virtual ΔT to an equivalent top drive rpm input, Ω_u , as shown in Fig. 3. The instantaneous value of Ω_u is evaluated using (9) with the virtual control ΔT applied as the input:

$$\frac{\dot{\alpha}_v(s)}{\Delta T(s)} = \frac{sd}{s^2 + sb + c}, \quad (9)$$

and then numerically integrated to obtain $\dot{\alpha}_v$. The angular velocity across the drillstring $\dot{\alpha}_v$ is then superimposed on the steady top drive rpm, Ω_r , to give the total instantaneous Ω_u such that in the steady state $\omega \rightarrow \Omega \rightarrow \Omega_r$.

4.1 Top-drive servo control design

The top-drive is controlled such that the stick/slip mitigating control input Ω_u can be tracked by the inner loop top-drive servo control system. The top-drive servo control is designed using pole placement where the open-loop drillstring plant is taken as (4) with the stiffness term set to zero and the state variable taken as the common angular displacement and velocity of the whole drillstring θ_c and $\dot{\theta}_c$, respectively. Hence the open-loop transfer function between the torque applied at the top drive and the common mode angular velocity of the whole drillstring can be derived as a first order lag assuming $\dot{\alpha} \rightarrow 0$, hence $\dot{\theta}_c \equiv \Omega \equiv \omega$, under the action of the stick/slip control in the steady state, therefore:

$$\ddot{\theta}_c + b\dot{\theta}_c = dT_{drive} \rightarrow \frac{\dot{\theta}_c(s)}{T_{drive}(s)} = \frac{d}{s+b}. \quad (10)$$

With these dynamics in mind, using a PI nested controller architecture similar to Fig. 5 but without the slow pole output stage, pole placement can be used to obtain the following proportional and integral gain expressions:

$$K_p = \frac{\omega_{n2}^2}{d}, \quad K_i = \frac{2\zeta\omega_{n2} - b}{d}, \quad (11)$$

for the closed loop transfer function:

$$\frac{y(s)}{r(s)} \equiv \frac{K_i d}{s^2 + s(b + dK_p) + K_i d}, \quad (12)$$

where d and b are the same parameters listed in Section 2.3 and are the parameters identified online for the stick/slip mitigation. In (11) ω_{n2} and ζ are the closed-loop natural frequency and damping ratio design constraints for the top-drive servo control pole placement.

5. RLS ALGORITHM

As per Astrom and Wittenmark (1994) the RLS algorithm minimizes a least square function for the parameter set θ :

$$V(\theta, k) = \frac{1}{2} \sum_{i=1}^k (z(i) - \phi^T(i)\theta)^2, \quad z(i) = \phi^T(i)\theta. \quad (13)$$

where θ is the vector of coefficients $(b, c, d)^T$ as defined in Section 2.3. It can be shown that the online recursive algorithm that minimizes this function is of the form:

$$K(k) = \frac{P(k-1)\phi(k)}{\lambda + \phi^T(k)P(k-1)\phi(k)},$$

$$P(k) = \frac{[I - K(k)\phi^T(k)]P(k-1)}{\lambda},$$

$$\theta(k) = \theta(k-1) + K(k)(z(k) - \phi^T(k)\theta(k-1)), \quad (14)$$

where k is the k^{th} recursion of the algorithm, z is the measured variable ($\ddot{\alpha}$ in this case), ϕ can be deduced to be vector $(-\alpha, -\dot{\alpha}, \Delta T)^T$, P is the covariance matrix for the vector ϕ , and λ is the forgetting factor to tune the speed of convergence of the RLS algorithm. The online identification algorithm requires all the states ($\ddot{\alpha}$, $\dot{\alpha}$, and α) and ΔT , requiring $\dot{\alpha}$, T_{bit} , and T_{drive} to be measured.

Note: For the RLS algorithm to be consistent such that the parameters converge to the true values then for the second order FIR (Finite-Impulse Response) model formulation used the inputs to the system must be PE (Persistently Exciting) of at least second order too (Astrom and Wittenmark 1994, Chapter 2, Section 2.4). Given that a sine wave is PE order 2, and that the open loop plant as a minimal modeling abstraction is equivalent to a torsional spring, inertia and damper system with one sinusoidal harmonic, then in reality the real system with many harmonics and near white noise excitation will easily satisfy the PE requirement.

6. IMPLEMENTATION IMPLICATIONS

Because the online identification and pole placement algorithm utilizes an assumed open-loop plant model with α and $\dot{\alpha}$ as states and ΔT as the input, then this implies ‘WDP’ uphole communications is available. WDP refers to a continuous electrical connection for communications with the tool downhole by means of a wire passed through each stand of the drillstring and inductively coupled at each threaded joint between stands. WDP is a relatively new technology, and for two-way communication RSS directional tools still, on the whole, utilize mud pulse telemetry with bandwidths of a few bits per second, which would not be anywhere near sufficient for this application.

Assuming a bandwidth of the drillstring stick/slip oscillation of up to 10 Hz, this implies the update rate for the ω and T_{bit} downhole transducers should be at least 100 Hz. One solution would be to measure and signal condition ω and T_{bit} downhole at the 100 Hz or more update rate and communicate their signal processed value to the surface via WDP at a lower update rate, and implement the adaptive stick/slip control algorithm on the surface where Ω_u can be applied by the servo control. It is assumed that the signal conditioning applied to the down hole rate gyro and load cell transducers (for measuring ω and T_{bit} will be appropriately filtered and signal processed [to obtain $\ddot{\alpha}$]). The closed-loop bandwidths of the different parts of the system are dictated by the closed-loop bandwidth of the inner loop top-drive servo control, which using standard convention, is designed to be $\omega_{n2} = 2.5$ Hz due to the $\omega_{n1} = 0.05$ Hz design bandwidth of the outer loop stick/slip control system.

7. TRANSIENT SIMULATIONS

A transient simulation of the drillstring dynamics and control algorithm was created which used the architecture shown in Fig. 3. For all the simulations the parameter set and values given in Table 1 were used unless otherwise stated. The two simulations run were for a multi-stage drillstring model as per the state space equations given in Fig. 6 with and without stick/slip mitigation. These simulations show the stick/slip mitigation assuming a single stage drillstring model for adaptive controller design still works when applied to a more realistic drillstring transient model incorporating a series of torsional springs and dampers. In all cases, a random noise torque input signal was added to the torque-on-bit disturbance input with a Gaussian amplitude standard deviation as stated in Table 1 to allow for the effect of unmodeled dynamics in the system.

$$\mathbf{A} = \begin{bmatrix} 0 & 0 & 0 & 0 & 0 & 1 & 0 & 0 & 0 & 0 \\ 0 & 0 & 0 & 0 & 0 & 0 & 1 & 0 & 0 & 0 \\ 0 & 0 & 0 & 0 & 0 & 0 & 0 & 1 & 0 & 0 \\ 0 & 0 & 0 & 0 & 0 & 0 & 0 & 0 & 1 & 0 \\ 0 & 0 & 0 & 0 & 0 & 0 & 0 & 0 & 0 & 1 \\ -c & c & 0 & 0 & 0 & -b & b & 0 & 0 & 0 \\ c & -2c & c & 0 & 0 & b & -2b & b & 0 & 0 \\ 0 & c & -2c & c & 0 & 0 & b & -2b & b & 0 \\ 0 & 0 & c & -2c & c & 0 & 0 & b & -2b & b \\ 0 & 0 & 0 & c & -c & 0 & 0 & 0 & b & -b \end{bmatrix}$$

$$\mathbf{B} = \begin{bmatrix} 0 & 0 & 0 & 0 & 0 & \frac{1}{J} & 0 & 0 & 0 & 0 \\ 0 & 0 & 0 & 0 & 0 & 0 & 0 & 0 & \frac{1}{J} & 0 \end{bmatrix}^T \quad \mathbf{C} = \begin{bmatrix} 0 & 0 & 0 & 0 & 0 & 0 & 0 & 0 & 0 & 0 \\ \vdots & \vdots \\ 0 & 0 & 0 & 0 & 1 & 0 & 0 & 0 & -1 \\ 0 & 0 & 0 & 0 & 1 & 0 & 0 & 0 & 0 \end{bmatrix}$$

$$\mathbf{D} = [0, 0, 0, 0, 0, 0, 0, 0, 0, 0]^T$$

Fig. 6. State space matrices for multistage torsional spring and damper drillstring model.

7.1 Transient simulation results

No stick/slip mitigation, This simulation is for the case where the simulation is started with a steady top drive rpm and the stick/slip oscillations allowed to build up in the absence of mitigating stick/slip control. Fig. 7 shows that without stick/slip mitigation in the steady state substantial oscillations in T_{bit} with a nominal value

of 3000 Nm occur. Also from Fig. 8, in the absence of stick/slip mitigation oscillations rapidly build up until after 30 seconds the stick/slip exceeds 100% (i.e, the peak angular speed is more than twice the mean angular speed) and the bit actually periodically stops. It can be seen in Fig. 8 that the nominal bit rpm is 230, resulting in a nominal V_{ROP} of 200 ft/hr. Note that in Fig. 8 the bit rpm and V_{ROP} are in phase.

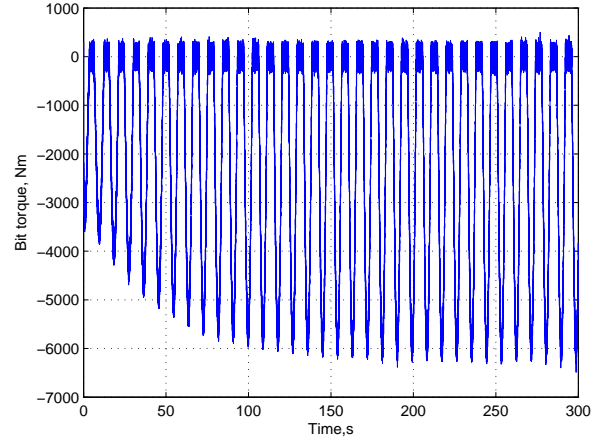


Fig. 7. T_{bit} with no stick/slip mitigation.

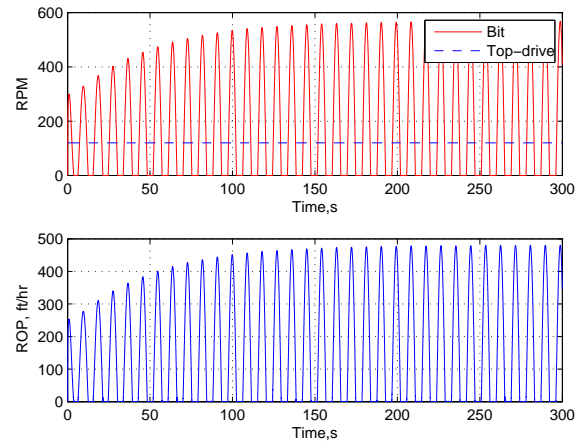


Fig. 8. Bit RPM & V_{ROP} with no stick/slip mitigation.

With stick/slip mitigation, Figs 9, 10, and 11 show the same test case but with the stick/slip mitigation control enabled from zero seconds. However, due to the sample and hold on the pole placement design utilizing the RLS identified parameters, the stick/slip mitigation controller has little effect until after the first sample-and-hold update at 50 seconds, with the stick/slip oscillation being identical to that seen with no stick/slip mitigation up until this point. This is because the initialized parameters in the pole placement online design are deliberately set to give small gains until the RLS algorithm has recurred enough to converge to the correct parameter values, and hence giving reasonable pole placed gains. It can be seen in Figs 9 and 10 that after 50 seconds as the fully converged identified parameters are used, the stick/slip oscillations are reduced until after 200 seconds the oscillations in ω , V_{ROP} and

torque on bit approach steady values of 120 rpm, 100 ft/hr, and -1400 Nm, respectively. It can also be seen in Fig. 11 that the RLS identified parameters have convincingly converged by the time of the first sample-and-hold update at 50 seconds.

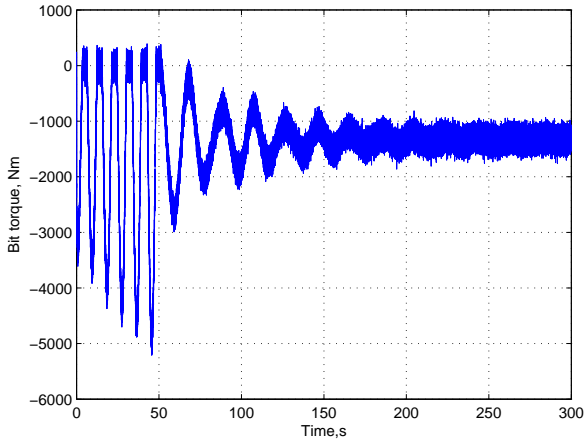


Fig. 9. T_{bit} with stick/slip mitigation.

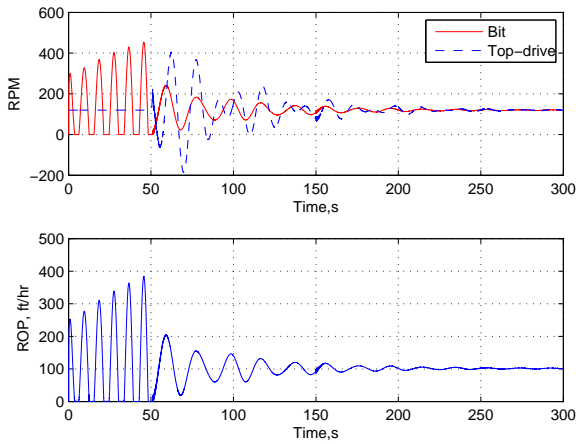


Fig. 10. Bit RPM and V_{ROP} with stick/slip mitigation.

8. CONCLUSION

In this paper the most important dynamics for the RSS phenomenon of stick/slip are summarized to be the the second order lag representing α with ΔT as a virtual control input. For the stick/slip mitigation, an online pole placement design utilizing a derivative and integral nested architecture with an additional zero canceling slow pole is then implemented in conjunction with a standard RLS forgetting factor algorithm and output stage evaluating Ω_u equivalent to the required differential torque across the drillstring. The physical control input from the stick/slip mitigation controller, i.e., Ω_u , is then tracked by a servo control system for the top-drive, the online parameter identified and pole placed design for which is also described and simulated in the paper. The paper therefore describes a coupled adaptive algorithm for stick/slip mitigation and top-drive servo control that by simulation is shown

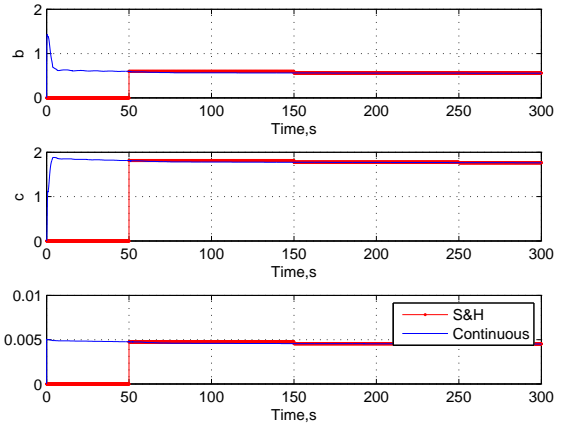


Fig. 11. RLS identified parameters with stick/slip mitigation.

to be robust to the unmodeled dynamics (these include the bit characteristics, random torsional disturbances at bit, and multistage drillstring dynamics) and parameter uncertainty in the sense that the online pole placement designs utilize online identified system parameters.

REFERENCES

- F. Abbassian and V. A. Dunayevsky. Application of stability approach to torsional and lateral bit dynamics. *SPE Drilling and Completion*, 13(2):99–107, 1999.
- K. J. Astrom and B. Wittenmark. *Adaptive Control*. Addison Wesley, second edition, 1994.
- J. F. Brett, T. M. Warren, and S. M. Behr. Bit whirl - a new theory of PDC bit failure. *SPE Drilling Engineering*, 5(4):275, 1990.
- E. Detourney, T. Richard, and M. Shepherd. Drilling response of drag bits, theory and experiment. *International Journal of Applied Mechanics & Mining Sciences*, 45:1347–1360, 2008.
- A. Hatch, N. Shepherd, and P. Diepeveen. Managing new technology introduction to provide maximum benefit. *SPE/IADC*, 140391, 2011.
- L. Lin, Q. Zhang, and N. Rasol. Time varying sliding mode adaptive control for rotary drilling system. *Journal of Computers*, 6(3):564–570, 2011.
- E. M. Navarro-Lopez and D. Cortes. Sliding-mode control of a multi-DOF oilwell drillstring with stick-slip oscillations. In *Proceedings of the 2007 American Control Conference New York City, USA, July 11 -13, 2007*.
- J. Rudat and D. Dashevskiy. Development of an innovative model-based stick/slip control system. *SPE/IADC*, 139996, 2011.
- A. F. A. Serrarens, M. J. G. van de Molengraft, J. J. Kok, and L. van den Steen. \mathcal{H}_∞ control for suppressing stick-slip in oil well drillstrings. *IEEE Control Systems Magazine*, 18:19–30, 1998.
- R. W. Tucker and C. Wang. On effective control of torsional vibrations in drilling systems. *Journal of Sound and Vibrations*, 224(1):101–122, 1999.